IJME

Int. J. of Applied Mechanics and Engineering, 2025, vol.30, No.1, pp.112-126
DOI: 10.59441/ijame/197391

COMPLEX DYNAMICS OF A HEAVY SYMMETRICAL GYROSCOPE UNDER A PARAMETRIC NONLINEAR DAMPING

G.F. Pomalegni[1,2], Y. Nourou[2], C.H. Miwadinou[*2,3] and A.V. Monwanou[2]

[1]Ecole de Génie Rural, Université Nationale d'Agriculture, Kétou, BENIN
[2]Laboratoire de Mécanique des Fluides, de la Dynamique Non Linéaire et de la Modélisation des Systèmes Biologiques (LMFDNMSB), Institut de Mathématiques et de Sciences Physiques, Porto-Novo, BENIN
[3]Département de Physique, ENS-Natitingou, Université Nationale des Sciences, Technologies, Ingénierie et Mathématiques (UNSTIM) Abomey, BENIN
E-mail: clement.miwadinou@imsp-uac.org

This paper analyzes the chaos and coexistence of attractors of a heavy gyroscope with parametric nonlinear damping. After having found the mathematical model of the dynamics, we used the multiple scale technique to look for secondary resonances. Subsequently, the amplitude of the harmonic oscillations is determined based on the harmonic balance technique. Impact of each of the system parameters is analyzed on the amplitudes and frequency of resonances. By applying order four Runge-Kutta algorithm, the different dynamics of the gyroscope are determined and analyzed. Subharmonic resonances and harmonic oscillations are derived from the limited development the basic equation solved numerically to investigate the dynamics and coexistence of the gyroscope attractors. The analysis of impact of each parameter on the existence and disappearance of coexisting attractors is done numerically.

Key words: parametric nonlinear damping, sub-harmonic resonances, gyroscope, coexistence of attractors, chaos.

1. Introduction

Studying gyroscope behavior, a captivating field of nonlinear dynamics, is rooted in a rich history of more than a century. Gyroscopes, thanks to their ability to model a multitude of physical systems in fields as varied as navigation, aeronautics and space engineering, have attracted the attention of numerous researchers over the decades [1]. This fascination with gyroscopic movements has encouraged several authors to deepen the study of their dynamics. For example, in 1996, Ge and Chen [2] as well as Ge *et al.* [3] explored the nonlinear dynamics of a heavy symmetrical gyroscope mounted on a vibrating base, highlighting the chaotic movements resulting from the gyroscopic system subjected to linear damping. In 2001, Tong and Mrad [4] examined the movement of a symmetrical gyroscope, under the effect of a basic vertical harmonic excitation, without taking into account certain parameters. The various works have demonstrated that gyroscopes are not spared from the complex phenomena common in nonlinear dynamics, such as nonlinear resonances, chaos, coexistence of attractors, amplitude jumps, hysteresis and nonlinear parametric damping [5]. These phenomena, which manifest themselves in a wide range of mechanical [6-10], biochemical [12], and industrial systems, make the prediction of the position and velocity of these systems in time and space particularly difficult [13-34].

Faced with these challenges, various control methods are employed in nonlinear dynamics, including active, semi-active, passive control, as well as feedback control [5-34]. For example, recently, the passive control of chaos and multistability of a non-linear damped gyroscope was achieved, demonstrating that these phenomena are better controlled when the gyroscope vibrates in the opposite direction to the vibrating rod on

[*] To whom correspondence should be addressed

which it is fixed. [5]. Likewise, the effect of biharmonic excitation on the dynamics and coexistence of gyroscope attractors, whose behavior is governed by a system of three differential equations, was studied [34]. The authors concluded that the dynamics of the gyroscope is strongly influenced by the frequencies of the biharmonic force, thus confirming the impact of its vibrational environment on its behavior, as previously demonstrated [5] .

In nature, systems that escape the influence of at least one damping force are rare. Extensive research has been conducted on the impact of damping forces, demonstrating that these dissipative forces play a significant role in chaotic dynamics and the coexistence of attractions. These dissipative forces were taken into account as a polynomial function. It is therefore obvious that gyroscopes are not spared by the action of a dissipative force, as certain authors have shown in their previous work [2-4, 14, 15, 26-33]. Recently, Kpomahou and his collaborators also demonstrated that parametric dissipative forces can influence the dynamics of complex systems [34-36].

Their conclusion shows that increasing the amplitude of the parametric damping force favors the regular behavior of the system. To date, there are no studies in the literature concerning the impact of a nonparametric damping force on the complex gyroscope vibrations. We therefore, based on this motivation, researched the influence of a parametric linear damping force on the complete phenomena of the gyroscope [37]. In light of the significant results we have obtained, we have recognized the necessity and importance of exploring the complex gyroscopes vibrations and controlling them by considering nonlinear parametric damping. Consequently, our proposal in this study is to search the dynamics of gyroscope when subjected to a non-linear parametric damping force. The main objective is to examine the impact of this nonlinear parametric damping force on the complex phenomena that the gyroscope can undergo.

The rest of the work is presented as: In section 2 the complex oscillations of the gyroscope are modeled. Section 3 identifies the different possible resonances, determines the harmonic solution and controls them. It also studies the impact of each system parameter, evaluated numerically. In section 4, chaos, coexistence of attractors are sought and controlled by the proposed damping force. Finally, the work ends with a conclusion.

2. Mathematic model of gyroscope dynamics

The system to be considered is a single-frequency-driven gyroscope model mounted on a vibrating base, as illustrated schematically in Fig.1. The motion of a symmetrical gyroscope mounted on a vibrating base can be described by Euler angles θ, ϕ and ψ .

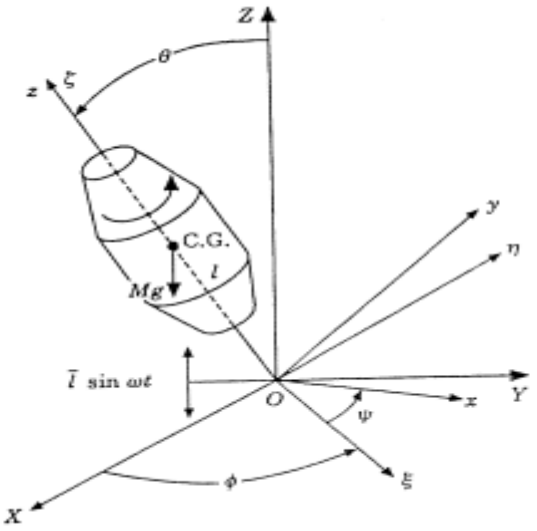

Fig.1. Schematic diagram of the single-frequency-driven gyroscope.

l - the distance between the center of gravity and O; $\bar{l}$ - the magnitude of the external excitation disturbance; Mg - the force of gravity; ω - the frequency of the external excitation disturbance; θ - nutation angle; ϕ - precession angle; ψ - rotation angle around the gyroscope's symmetry axis.
The Lagrangian of the system is written as follows [28]:

$$L=\frac{1}{2}I_1\left(\dot{\theta}^2+\dot{\phi}^2\sin^2\theta\right)+\frac{1}{2}I_3\left(\dot{\phi}\cos\theta+\dot{\psi}\right)^2-Mg\left(l+\bar{l}\sin\omega t\right)\cos\theta \tag{2.1}$$

with I_1 and I_3 - are the polar and the equatorial moments of inertia of the gyroscope, respectively.
From the analysis of Eq.(2.1), it is observed that ϕ and ψ represent cyclic coordinates. Thus, the first integrals are:

$$P_\phi=\frac{\partial L}{\partial\dot{\phi}}=I_1\sin^2\theta+I_3\left(\dot{\phi}\cos\theta+\dot{\psi}\right)\cos\theta=\beta_\psi, \tag{2.2}$$

$$P_\psi=\frac{\partial L}{\partial\dot{\psi}}=\left(\dot{\phi}cos\theta+\dot{\psi}\right)=\beta_\phi=I_3\omega_z. \tag{2.3}$$

We utilize to simplify the Routhian formulation:

$$R=L-P\phi\dot{\phi}-P\psi\dot{\psi}. \tag{2.4}$$

Depending on the nature of the medium with which the gyroscope interacts, the dynamics of the gyroscope can be influenced by damping forces [1-5]. Here, we consider the following parametric damping force [34, 35]:

$$F_d=\left(1+hcos\left(\omega t\right)\right)\left(\lambda\dot{\theta}+\gamma\dot{\theta}^3\right), \tag{2.5}$$

h is parametric damping amplitude λ and γ - coefficients describing respectively the linear and nonlinear damping of the system. The cubic nonlinear term $\gamma\dot{\theta}^3$ is added to capture the high-amplitude nonlinear effects commonly observed in mechanical systems where nonlinear deformations or behaviors occur at high amplitudes. A quadratic term was not considered as it does not adequately reflect the dynamics observed in this type of system, as discussed in the works of [36, 37].
The dynamic equation of the gyroscope is therefore:

$$\frac{d}{dt}\frac{\partial R}{\partial\dot{\theta}}-\frac{\partial R}{\partial\theta}=F_d. \tag{2.6}$$

Inserting Eq.(2.4) and Eq.(2.5) in Eq.(2.6), we obtain after some mathematical transformations:

$$\ddot{\theta}+\frac{\beta_\phi^2}{I_1^2}\frac{\left(1-\cos\theta\right)^2}{\sin^3\theta}+\left(1+h\cos\omega t)(\lambda\dot{\theta}+\gamma\dot{\theta}^3\right)-\frac{Mgl}{I_1}\sin\theta=\frac{Mg}{I_1}\bar{l}\sin\omega t\sin\theta. \tag{2.5}$$

Thus, we have

$$\ddot{x}+\alpha^2\frac{\left(1-\cos\left(x\right)\right)^2}{\sin^3\left(x\right)}+\left(1+h\cos\left(\omega t\right)\right)\left(\lambda\dot{x}+\gamma\dot{x}^3\right)-\beta\sin\left(x\right)=f\sin\left(\omega t\right)\sin\left(x\right) \tag{2.6}$$

with $$x=\theta,\quad \alpha=\frac{\beta_\varphi}{I_1}=\frac{I_3\,\omega_z}{I_1},\quad \beta=\frac{Mgl}{I_1},\quad f=\frac{Mg}{I_1}\bar{l}. \tag{2.7}$$

3. Gyroscope resonant states and harmonics oscillations

To understand the overall behavior of a nonlinear dynamic system, it is important to determine its resonance states. Thus, the resonance amplitudes are determined and consequently the mechanical energy of the system could be controlled because it is proportional to the square of the amplitude of the vibrations [8-14]. Indeed, an exaggerated increase in energy at resonance in mechanical systems can cause excessive vibration, fatigue of materials, breakage, etc. of the system. To know the vibration amplitude ranges and avoid this damage to gyroscopic systems, this section detects the resonance states of the gyroscope and analyzes the influences on these resonances.

In order to be able to analytically determine the possible resonance states of the gyroscopes and taking into account the strong nonlinearity of the dynamic equation, we take the limited expansion of $\sin x$ and $\frac{(1-\cos(x))^2}{\sin^3(x)}$ at order 3 gives $\sin x = x-\frac{1}{6}x^3$ and $\frac{(1-\cos(x))^2}{\sin^3(x)}=\frac{1}{4}x+\frac{1}{12}x^3$.

Using these limited expansions, Eq.(2.8) becomes:

$$\ddot{x}+\omega_0^2 x=-\mu x^3+(1+h\cos\omega t)\left(\lambda\dot{x}+\gamma\dot{x}^3\right)+f\sin\omega t\left(x-\frac{1}{6}x^3\right), \tag{3.1}$$

with $$\omega_0^2=\frac{\alpha^2}{4}-\beta,\quad \mu=\frac{\alpha^2}{12}+\frac{\beta}{6}.$$

In the following, we take $\omega_0^2=1$.

To identify subharmonic resonances, we employ the multiple-scale method.

Generally, the solutions are:

$$x(\varepsilon,t)=x_0(t_0,t_1,\ldots)+\varepsilon x_1(t_0,t_1,\ldots) \tag{3.2}$$

and the derivative operators can now be expressed as follows:

$$\frac{d^m}{dt^m}=\epsilon^n\frac{d^m}{dt_n^m}=\epsilon^n\partial_{t_n}^m, \tag{3.3}$$

$$\partial t=\partial_{t_0}+\varepsilon\partial_{t_1}+\ldots, \tag{3.4}$$

$$\partial_t^2=\partial_{t0}^2+2\varepsilon\partial_{t_0}\partial_{t_1}+\ldots, \tag{3.5}$$

with $t_n=\varepsilon^n t$ and $0\le\varepsilon\le 1$

By replacing Eqs (3.3), (3.4) and (3.5) in Eq.(3.1), we obtain: For ε^0 we have:

$$D_0^2 x_0+x_0=0 \tag{3.6}$$

and for ε^1, we have:

$$D_1^2 x_1 + x_1 = -2D_0 D_1 x_1 - \mu x_0^3 - \left(1 + h\cos(\omega T_0)\right)\left(\lambda D_0 x_0 + \gamma (D_0 x_0)^3\right) + \\ + f\sin(\omega T_0)\left(x_0 - \frac{1}{6}x_0^3\right). \tag{3.7}$$

The solutions of Eq.(3.6) are:

$$x_0 = A(T_1)e^{iT_0} + cc\,, \tag{3.8}$$

where *cc* denotes the complex conjugate terms.
Upon inserting x_0 into Eq.(3.7), we obtain:

$$D_0^2 x_1 + x_1 = -\left[2iA' - 3A^2\bar{A} - i\lambda A - 3\gamma A^2\bar{A}\right]e^{iT_0} - \left[\frac{h\lambda\bar{A}}{2} + \frac{i3h\gamma A\bar{A}^2}{2} + \right. \\ \left. + \frac{if\bar{A}}{2} + \frac{ifA\bar{A}^2}{4}\right]e^{i(\Omega-1)T_0} + \left[\frac{if\bar{A}^3}{12} + \frac{i3h\gamma A\bar{A}^3}{2}\right]e^{i(\Omega-3)T_0} + NST + cc. \tag{3.9}$$

NST and *cc* denote no secular and complex conjugate terms respectively. According to the analysis of Eq.(3.9), we see that, the nonlinear gyroscopes can only undergo subharmonic resonances such as $\Omega = 2 + \epsilon\sigma$ and $\Omega = 4 + \epsilon\sigma$, where σ is detuning parameter. The 2nd order subharmonic resonance $(\Omega = 2 + \epsilon\sigma)$ is treated in subsection 3.1 while the 4th order subharmonic resonance $(\Omega = 4 + \epsilon\sigma)$ is studied in subsection 3.2. Subsection 3.3 is dedicated to the harmonic vibrations of the gyroscope.

3.1. Subharmonic resonance order 2

This part determines the amplitude and frequency of the order 2 subharmonic resonance. For that, we insert $\Omega = 2 + \epsilon\sigma$ into Eq.(3.9), when the secular terms equal to *0* and we use:

$$A = \alpha(T_1)e^{T_1}. \tag{3.10}$$

Then, we obtained:

$$\alpha' = -\frac{\lambda\alpha}{2} - \frac{3\gamma h\alpha^3}{8} - \left(\frac{h\lambda\alpha}{2} + \frac{3h\gamma\alpha^3}{8} + \frac{f\alpha}{2} + \frac{f\alpha^3}{4}\right)\cos\nu, \tag{3.11}$$

$$\phi'\alpha = -\frac{3\mu\alpha^3}{8} - \left(\frac{h\lambda\alpha}{2} + \frac{3h\gamma\alpha^3}{8} + \frac{f\alpha}{2} + \frac{f\alpha^3}{4}\right)\sin\nu, \tag{3.12}$$

where $\kappa = \sigma T_1 - 2\phi$. Considering $a' = \kappa' = 0$, the second-order subharmonic resonance is:

$$\left(\frac{\lambda}{2} + \frac{3\gamma h\alpha^2}{8}\right)^2 + \left(\frac{\sigma}{2} - \frac{3\mu\alpha^2}{8}\right)^2 = \left(\frac{h\lambda}{2} + \frac{3h\gamma\alpha^2}{8} + \frac{f}{2} + \frac{f\alpha^2}{4}\right)^2. \tag{3.13}$$

The vibration amplitudes for the second order subharmonic resonance are completely determined by Eq.(3.13). Indeed, using the dichotomy method, we numerically determine the different amplitudes A of vibrations. Thus, Figures 2a, b, c obtained, show the impact of f, μ and λ respectively on this resonance. As for Figs 3a, b they show the effects of γ and h on the resonance. We see that the amplitude and σ increase when f, μ and λ increase while the amplitude and σ decrease with γ and h. It follows that the amplitude and the resonance frequency increase with the amplitude f of the excitation force, the coefficient μ of the nonlinear term of order 3, of the linear parametric dissipation but decrease when the nonlinear dissipation increases.

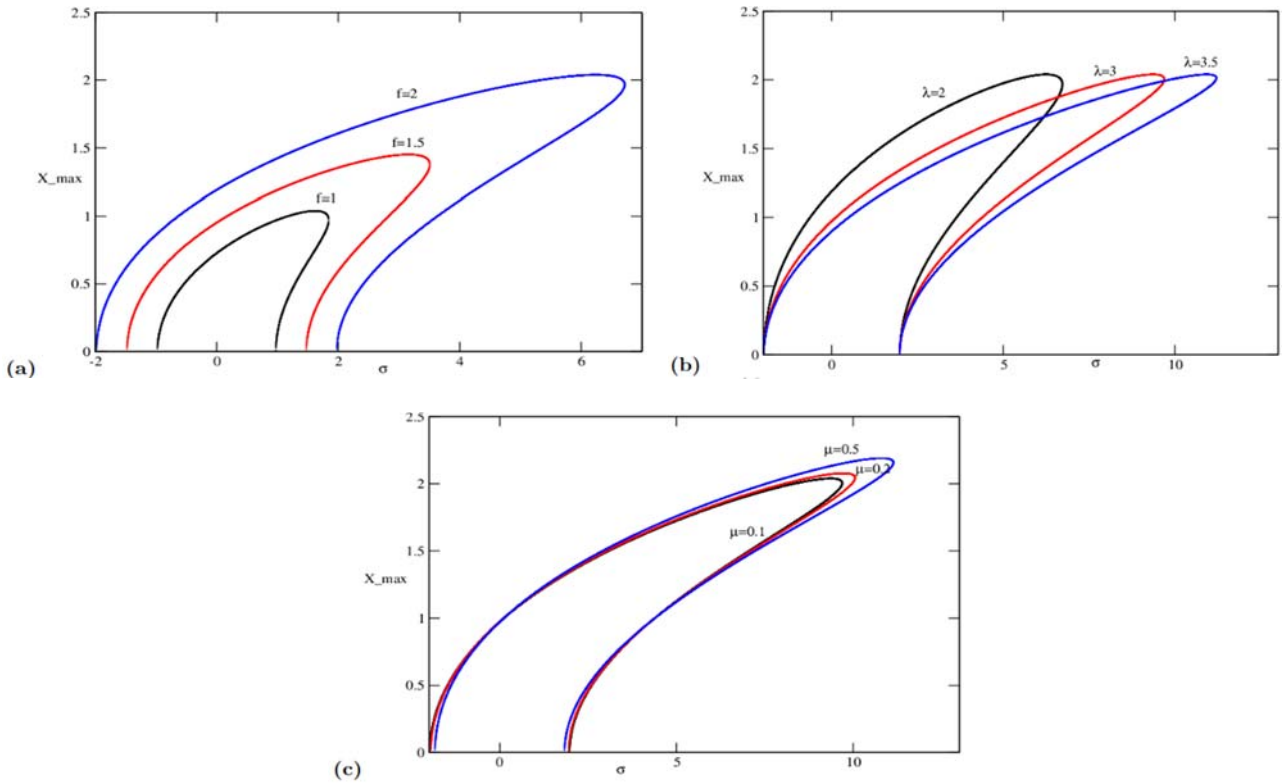

Fig.2. (a) Influence of parametric amplitude f, (b) Impact of parametric amplitude λ and (c) impact of parametric amplitude μ on order 2 subharmonic resonance curve when $\gamma=5$, $h=-0.2$, $\lambda=2$, $\mu=0.1$, $f=2$.

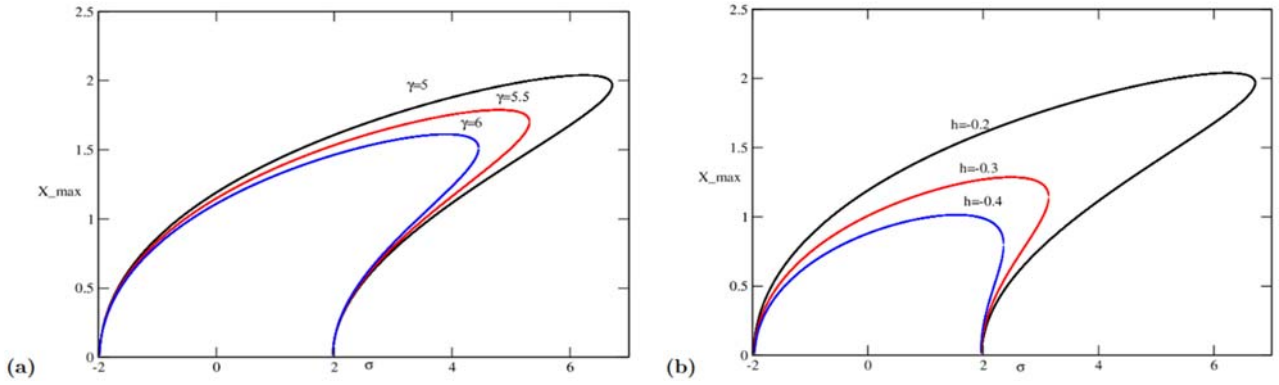

Fig.3. (a) Impact of γ and (b) impact of h on subharmonic resonance state in order 2 curve with $\lambda=2, h=-0.2, f=2, \mu=0.1, \gamma=5$.

3.2. Subharmonic resonance order 4

In this part, we studied the order 4 subharmonic resonance state. For this subharmonic state, $\Omega = 4 + \epsilon\sigma$. Equating resonance terms at *0* from Eq.(3.9), we obtained after some algebraic manipulations:

$$\alpha' = -\frac{\lambda\alpha}{2} - \frac{3\gamma h\alpha^3}{8} - \left(\frac{h\gamma\alpha}{2} + \frac{f\alpha^3}{12}\right)\cos\nu, \qquad \phi'\alpha = -\frac{3\mu\alpha^3}{8} - \left(\frac{h\gamma\alpha}{2} + \frac{f\alpha^3}{12}\right)\sin\nu, \tag{3.14}$$

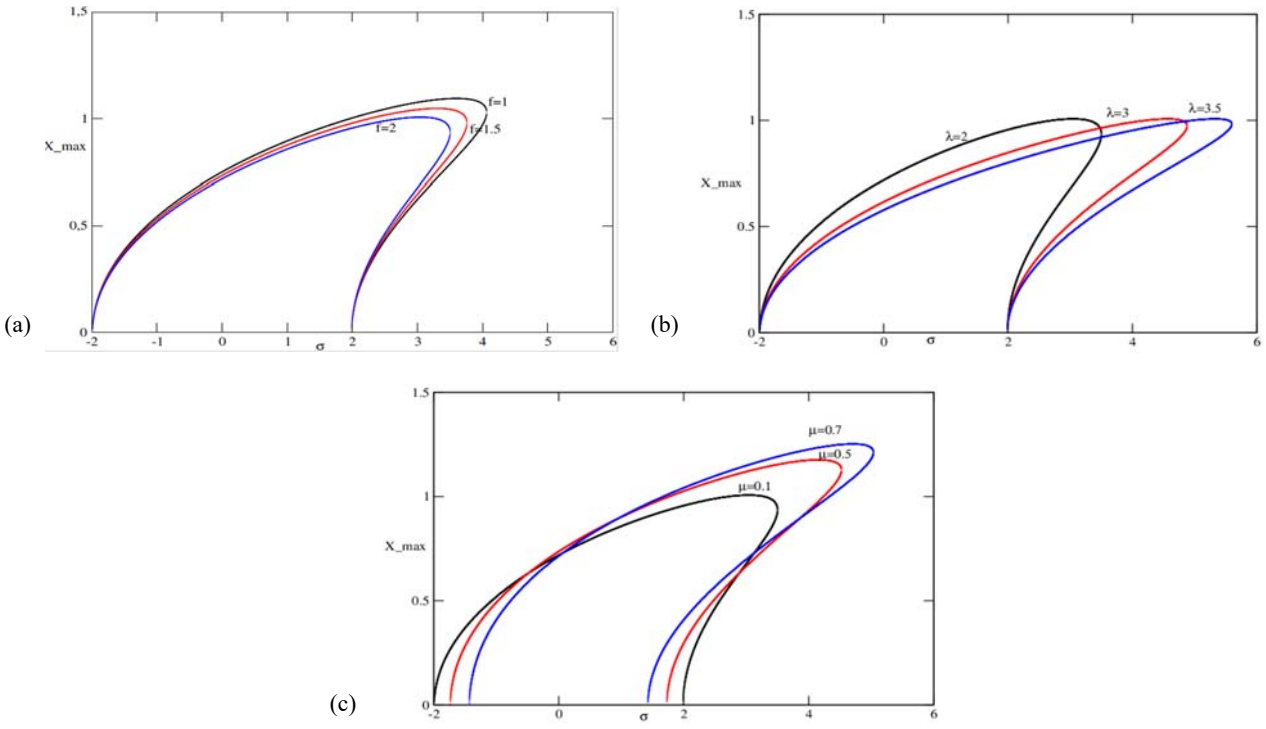

Fig.4. (a) Impact of parametric amplitude *f*, (b) Impact of λ and (c) Impact of μ on subharmonic resonance state in order 4 curve with $\gamma = 5,\ h = -0.2,\ \lambda = 2,\ \mu = 0.1,\ f = 2$.

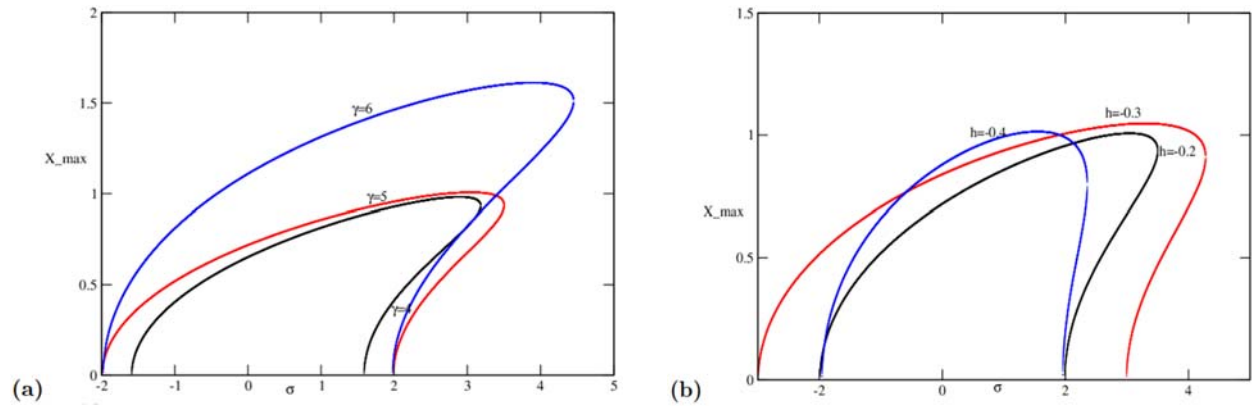

Fig.5. (a): Impact of γ and (b): Impact of *h* on subharmonic resonance order 4 with $\gamma = 5, f = 0.2, \mu = 0, h = 0.1, \lambda = 2$.

where $\eta=\sigma T_1-2\phi$. For $a'=\eta'=0$, the subharmonic resonance equation is:

$$\left(\frac{\lambda}{2}-\frac{3\gamma h\alpha^2}{8}\right)^2+\left(\frac{\sigma}{2}-\frac{3\mu\alpha^2}{8}\right)^2=\left(\frac{h\gamma}{2}+\frac{f\alpha^2}{12}\right)^2. \tag{3.15}$$

In the same way for the subharmonic resonance of order 4, Eq.(3.15) is solved by the dichotomy method. Figures 4a, b, c show us the impact of f, μ and λ respectively while for Figs 5a, b present the effects of γ and h. We see that the amplitude and σ increase when f, λ, μ, γ and h. It follows that the amplitude and the resonance frequency increase with the all system parameters.

3.3. Harmonic oscillations

To derive the amplitudes of harmonic vibrations of the gyroscope, we apply the harmonic balance method. Indeed, harmonic vibrations are determined by considering:

$$x(t)=A\cos\theta, \tag{3.16}$$

where $\theta=\omega t+\phi$. Let's substitute the harmonic solution into

$$\ddot{x}+x+\mu x^3-(1-h\cos\omega t)\left(\lambda\dot{x}+\gamma\dot{x}^3\right)=f\left(x-\frac{1}{6}x^3\right)\sin\omega t. \tag{3.17}$$

After some algebraic manipulations, we obtain:

$$\left(\frac{3A^2\omega^3\gamma}{4}+\omega\lambda+\frac{3A^2\omega^3\gamma h}{8}+\frac{h\omega\lambda}{2}\right)^2+\left(\omega^2+1+\frac{3\mu A^2}{4}-\frac{3hA^2\omega^3\gamma}{4}\right)^2=\left(f-\frac{1}{8}A^2\right)^2. \tag{3.18}$$

By solving this equation by the dichotomy method, we obtain the amplitudes of the harmonic vibrations and the results are represented by Figs 6 and 7. From these figures, we see that the amplitude and resonant frequency increase when λ, μ and h increase while the amplitude and resonant frequency decrease with γ and f.

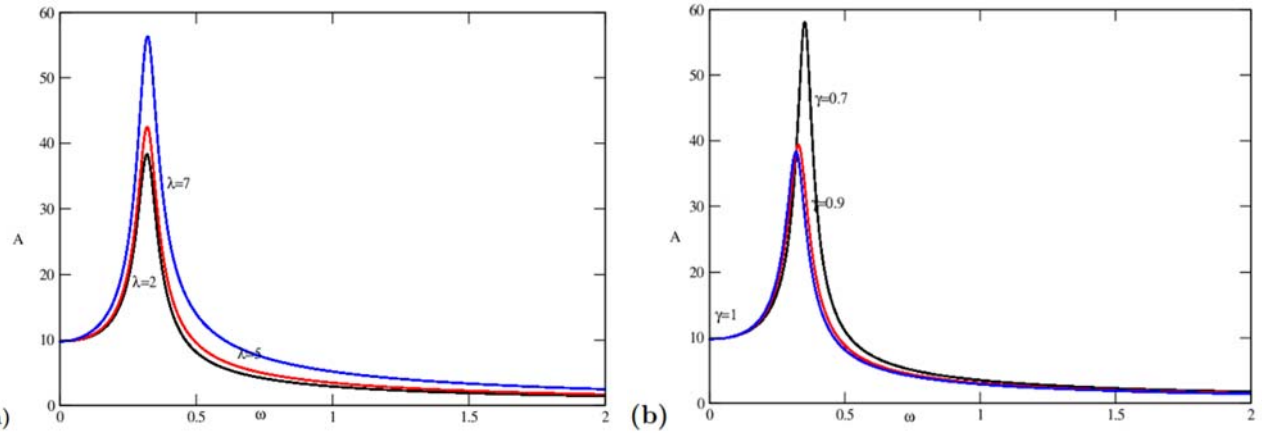

Fig.6. (a) Effect of λ, (b) effect of γ on the amplitude-frequency curve of the parameter when $\gamma=1$, $\mu=0.0$, $f=0.2$, $h=0.1$, $\lambda=2$.

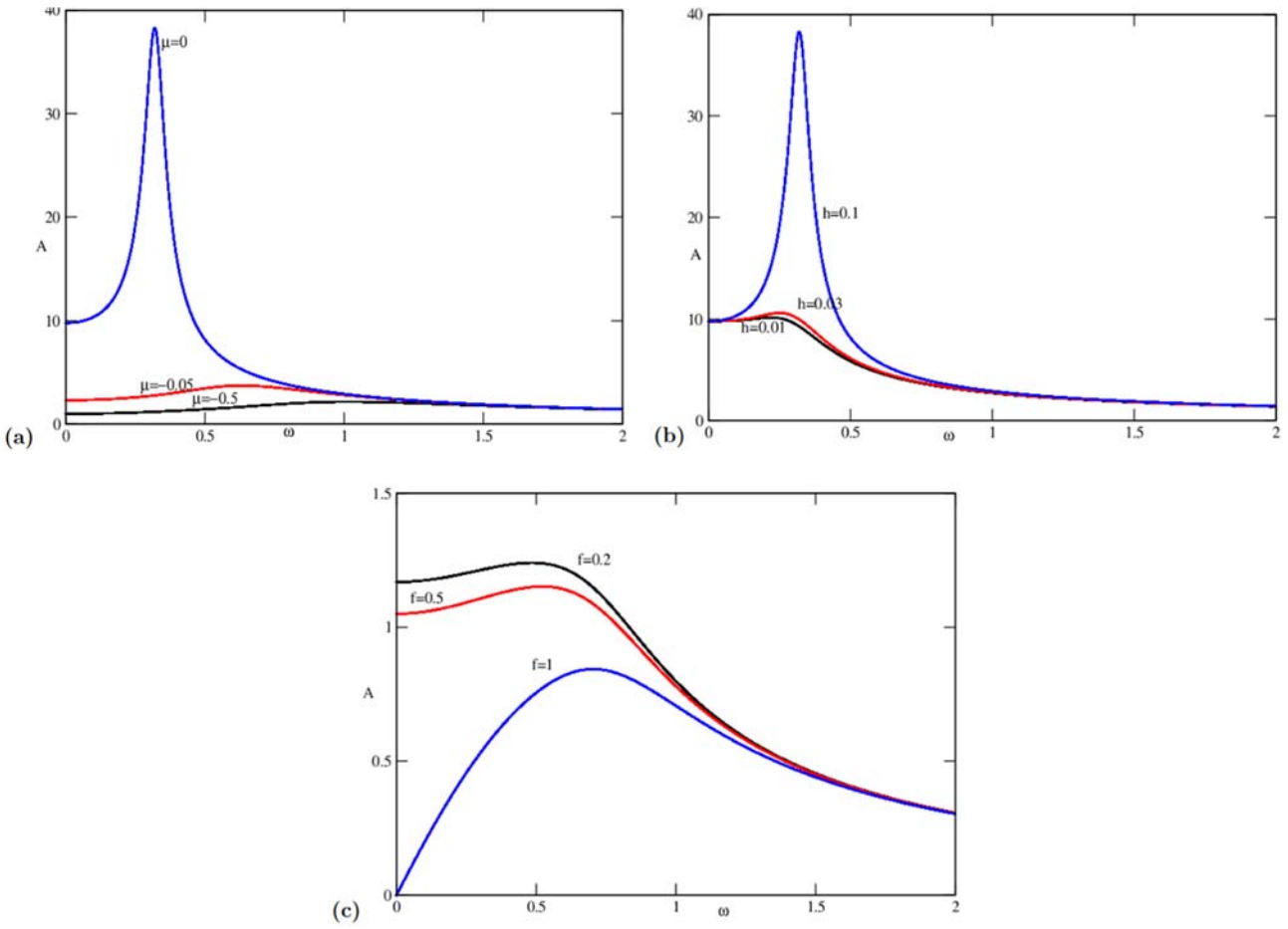

Fig.7. (a) Impact of μ, (b) effect of *h*, (c) Impact of f on the amplitude-frequency curve of the parameter with μ: $\gamma=1$, $\lambda=2$, $f=0.2$, $h=0.1$, $\mu=0.0$.

For Fig.7a, as μ increases (from *0* to *0.05* and then *0.5*) we observe that the peak decreases in amplitude and the curve tends to flatten.

4. Effect of a parametric nonlinear damping on chaotic dynamic and coexistence of attractors

Chaotic dynamics and the coexistence of attractors are very complex phenomena that can negatively affect the performance of the gyroscope because they do not guarantee stability in the movement of the gyroscope [5, 14, 15, 25]. This is the reason why Hounnan *et al.* [5] used passive control to eliminate both phenomena. Likewise Aguessivognon *et al.* [25] showed that when the gyroscope is under the influence of a biharmonic force, the chaotic dynamics and the coexistence of attractors can be accentuated or reduced depending on the appropriate values of the amplitude and frequency of the force biharmonic. Here we want to control the complex phenomena of the system using the nonlinear parametric dissipation force. To do this, we solve equation (2.8) numerically using the Runge-Kutta algorithm of order 4. For this, Eq.(2.8) is rewritten in the following form:

$$\dot{x}=y,\quad \dot{y}=-\alpha^2\frac{\left(1-\cos(x)\right)^2}{\sin^3(x)}-\left(1+h\cos(\omega t)\right)\left(\lambda y+\gamma y^3\right)+\beta\sin(x)+f\sin(\omega t)\sin(x). \quad (4.1)$$

For the simulations, the step for the bifurcation parameter is $hf = 0.001$; the step for time is $dt = 0.01$; the number of iterations is *1000000*; the initial conditions are: for the red curve $(x_0 = 0.5,\ y_0 = 0.2)$ and for blue curve $(x_0 = 0.5,\ y_0 = -0.2)$. Thus, taking h as a control parameter, the bifurcation diagram, the Lyapunov exponent as well as the phase space are represented. Figure 8 represents the bifurcation diagram and Lyapunov exponent obtained for h ranging from 9 to 14. From this figure, we see that the route to gyroscope chaos when the parametric damping varies is period-doubling. Figure 9, obtained for various values of h, shows phase portraits and confirms the bifurcation diagram prediction. Figures 10, 11, 12, 13 represent the bifurcation diagram for $9 \le h \le 14$ and show the impact of f, α, β and λ respectively on the coexistence of the attractors of the gyroscope complex vibrations. Figure 14 represents the phase portraits and confirmed the various attractors coexisting obtained at Fig.10. After all these analyses, we notice that the chaos and the coexisting attractors are strongly influenced by the control force and the parameters of the gyroscope.

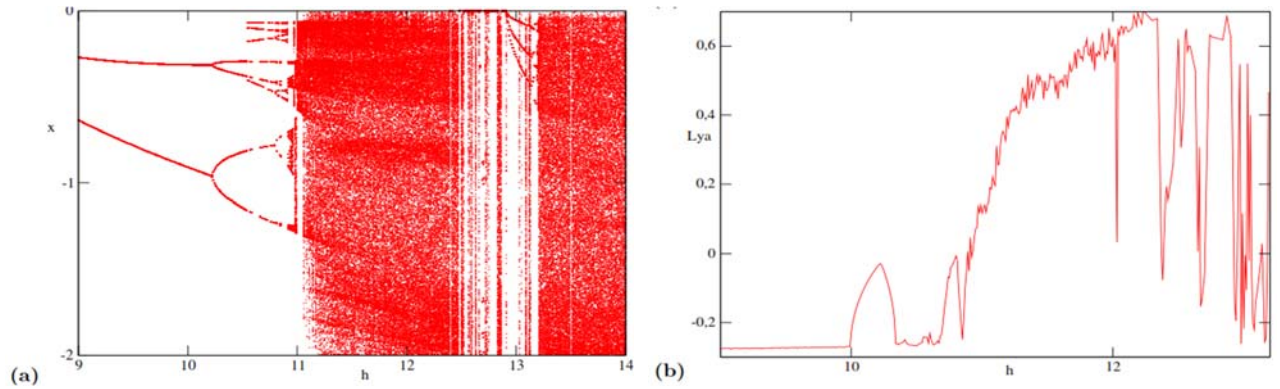

Fig.8. Bifurcation diagram and its corresponding Lyapunov exponent showing the route to chaos for the gyroscope when $\beta = 1$, $f = 40$, $\omega = 2$, $\gamma = 1$ and $\lambda = 1$.

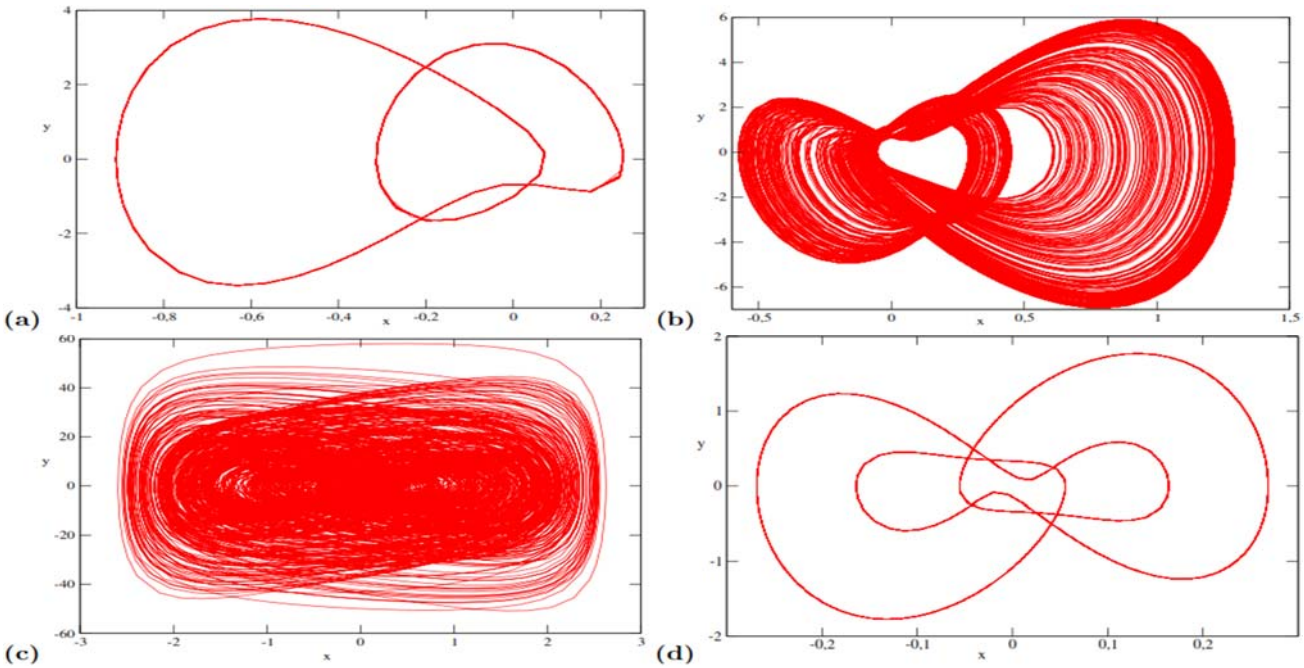

Fig.9. Phase portraits corresponding to (a) $h = 10$; (b) $h = 11.5$; (c) $h = 11$; $h = 12$ and (d) $h = 13$ using the parameters from Fig.8.

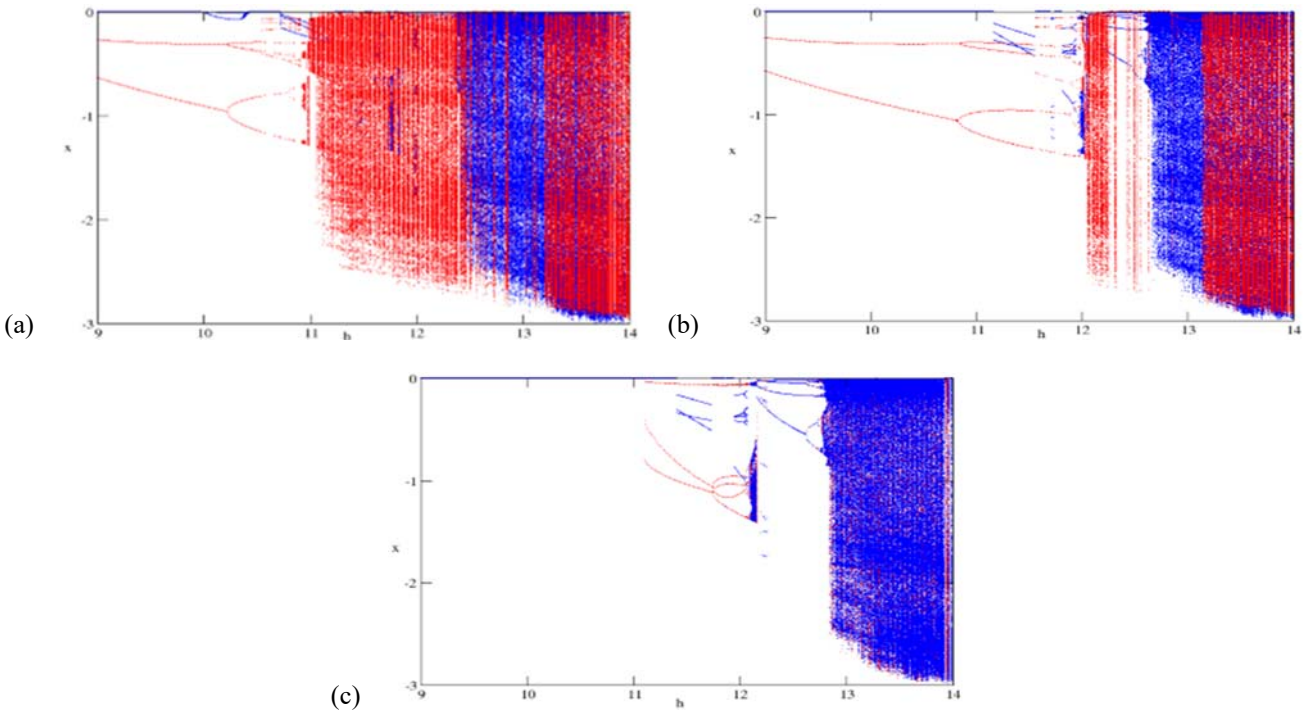

Fig.10. Dynamics and coexistence of the gyroscope for $\gamma=1$, $\lambda=1$, $\omega=2$ and $\beta=1$. Effect of f with $f=40$, $f=33.4$ and $f=33$ respectively for (a), (b) and (c). The red and blue curves are obtained for an increasing h (ranging from *9* to *14*) and decreasing h (ranging from *14* to *9*).

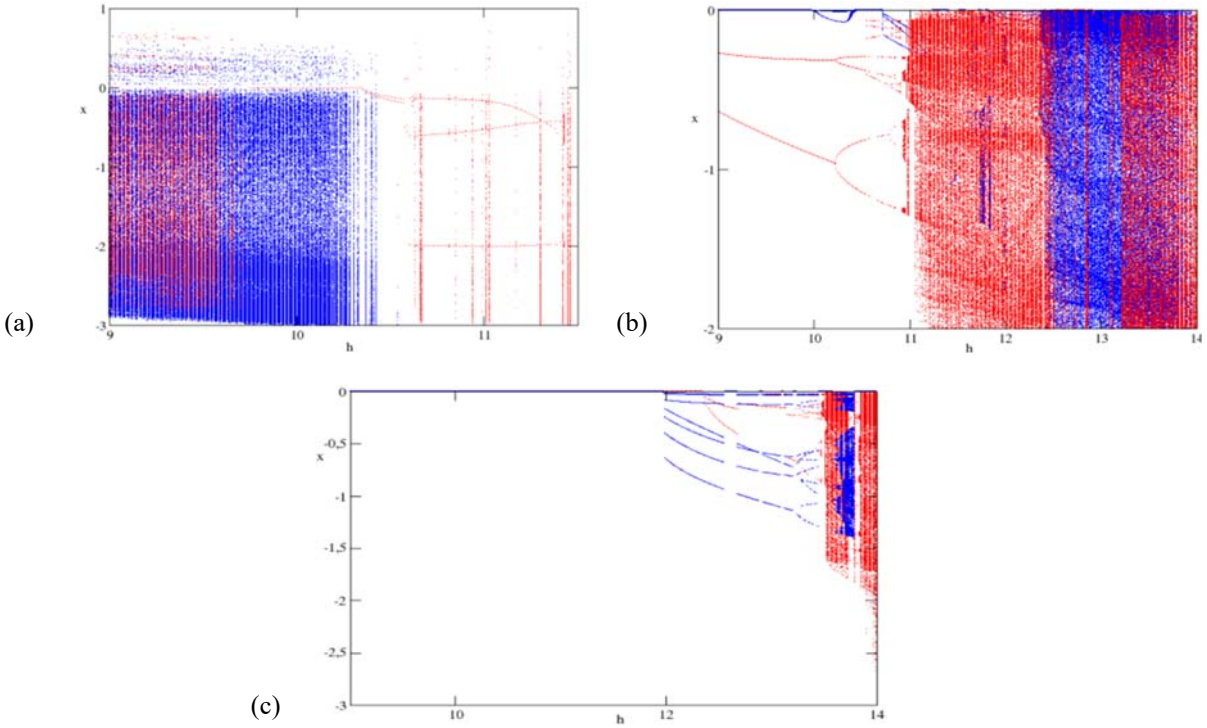

Fig.11. Effect of α on dynamics for $\gamma=1$, $h=0$, $\omega=2$ and $\beta=1$: (a) $\alpha=10$; (b) $\alpha=15$; (c) $\alpha=17$. The red and blue curves are obtained for an increasing h (ranging from *9* to *14*) and decreasing h (ranging from *14* to *9*).

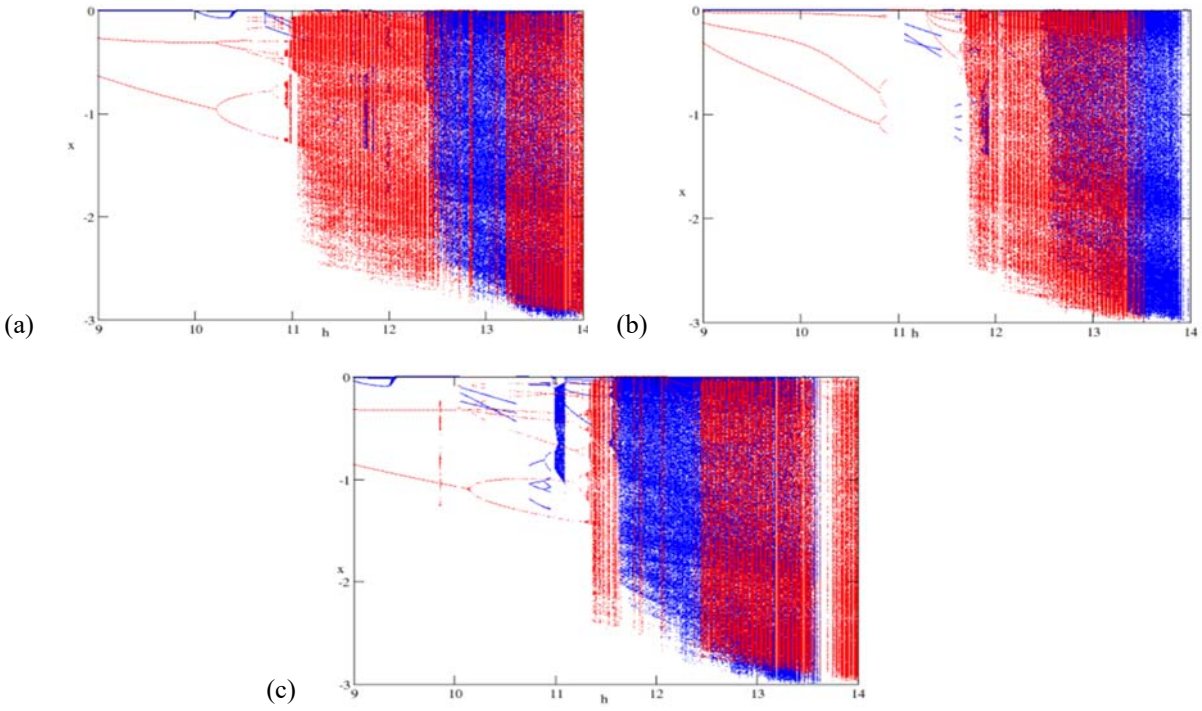

Fig.12. Impact of β on dynamics for $\gamma=1$, $\lambda=1$, $\omega=2$ and $\beta=1$, $f=40$: (a) $\beta=0.5$; (b) $\beta=1$; (c) $\beta=3.5$. The red and blue curves are obtained for an increasing h (ranging from *9* to *14*) and decreasing h (ranging from *14* to *9*).

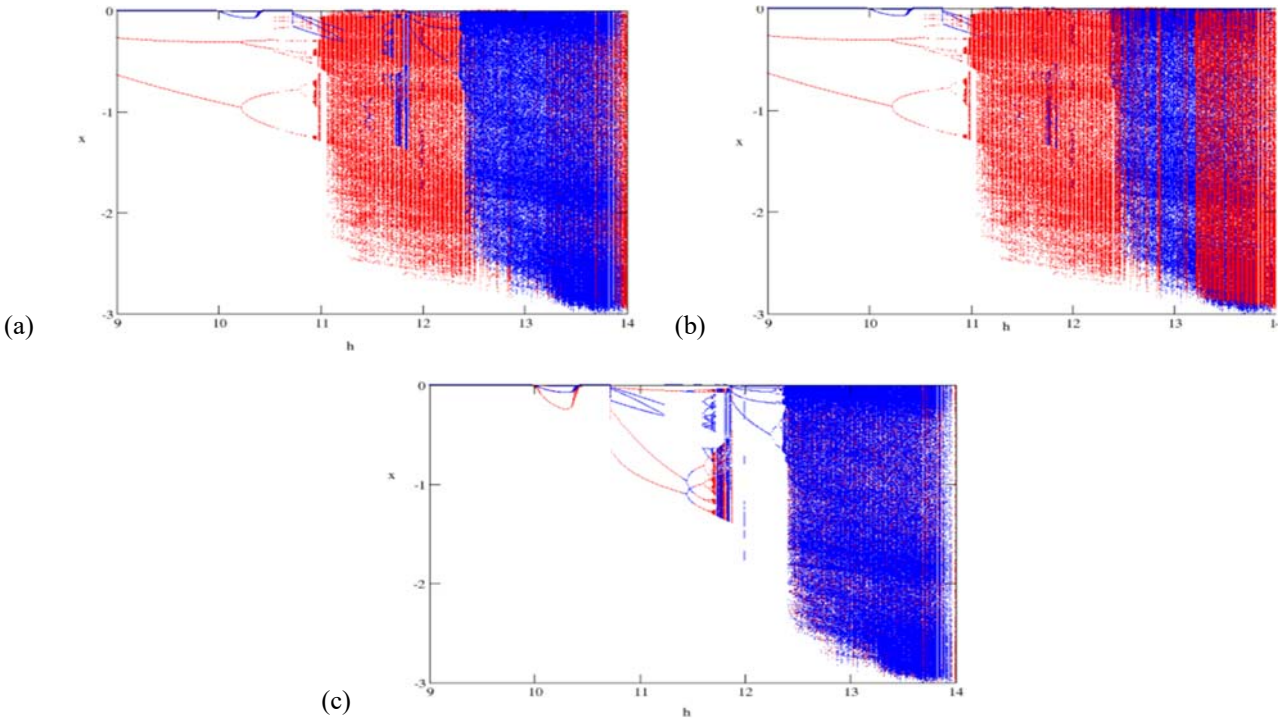

Fig.13. Effect of the parameter λ on dynamics for $\gamma=1$, $\omega=2$, $f=35$, $h=0$: (a) $\lambda=0$; (b) $\lambda=1$; (c) $\lambda=3.5$. The red and blue curves are obtained for an increasing h (ranging from *9* to *14*) and decreasing h (ranging from *14* to *9*).

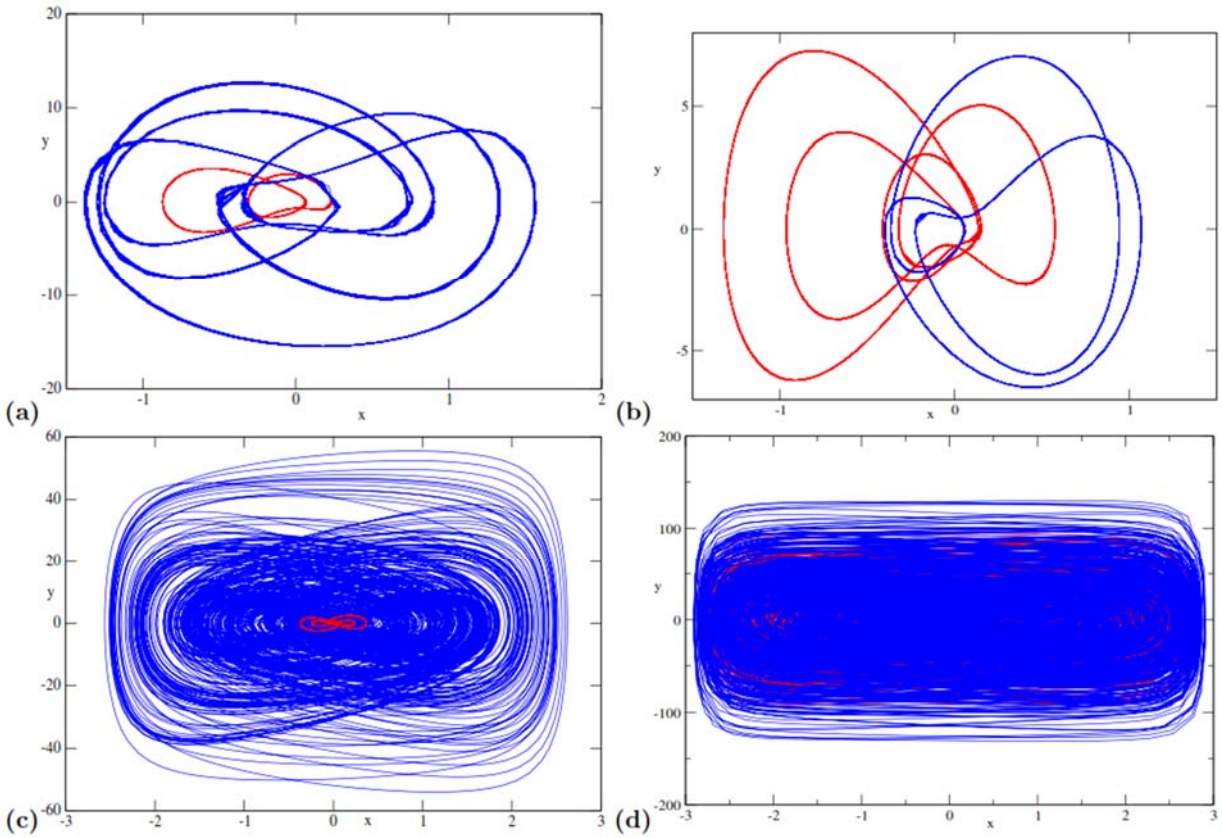

Fig.14. Phase portraits for (a) $h = 10$; (b) $h = 11.5$; (c) $h = 13$ and (d) $h = 13.5$ with the parameters of Fig.10. The red and blue curves are obtained for an increasing h (ranging from *9* to *14*) and decreasing h (ranging from *14* to *9*).

5. Conclusions

The impact of the non-linear damping force on the complex phenomena, secondary resonance, chaos and coexistence of attractors of a rotating gyroscope is studied in this work. From the Lagrangian of the system, the modeling of the non-linear dynamics is done. The multiple time scale technique is used to determine subharmonic resonances. We also used the harmonic balance method to determine the harmonic solution of the oscillator equation. The study of the impact of the parameters $\alpha, \beta, \gamma, \lambda, f$ and h on the resonances obtained. Subharmonic resonances exploit Eq.(3.9) while harmonic oscillations are obtained from Eqs (3.17) and the harmonic balance method. Equations (3.9) and (3.17) are derived from the limited development of Eq.(2.8) which is the basic equation solved numerically to investigate the dynamics and coexistence of the gyroscope attractors. We carried out numerical analyzes of the effects of these parameters on the complex dynamics of the system. As a result, the choice of the values of the system parameters impacts the chaotic dynamics and the coexistence of the system's attractors. Thus, we note that the chaotic dynamics and the coexistence of attractors can be eliminated for precise values of $\alpha, \beta, \gamma, \lambda, f$, h The growing advancement of rotating machinery technology widely used across various industrial sectors today necessitates an enhancement in both performance and efficiency of these machines based on their defining parameters.

Acknowledgments

The authors would like to thank very much the anonymous referees whose useful criticisms, comments and suggestions would helped strengthen the content and the quality of the paper.

Nomenclature

I_1, I_3 – the polar and the equatorial moments of inertia of the gyroscope, respectively

l – the distance between the center of gravity and O

$\overline{l}$ – the magnitude of the external excitation disturbance

Mg – the force of gravity

ω – the frequency of the external excitation disturbance

References

[1] Fuhong M. (2012): *Analysis of generalized projective synchronization for a chaotic gyroscope with a periodic gyroscope*.– Comm. Nonlinear Sci. Num. Sim., vol.17, pp.4917-4929.

[2] Ge Z.M., Chen H.K. and Chen H.H. (1996): *The regular and chaotic motions of a symmetric heavy gyroscope with harmonic excitation*.– J. Sound Vibr., vol.198, pp.131-147.

[3] Ge Z.M. and Chen H.K. (1996): *Stability and chaotic motion of a symmetric heavy gyroscope*.– Jpn. J. Appl. Phys., vol.35, pp.1954-1971.

[4] Tong X. and Mrad N. (2001): *Chaotic motion of a symmetric gyro subjected to a harmonic base excitation*.– J. Appl. Mech., vol.68, pp.681-684.

[5] Hounnan S.O., Miwadinou C.H. and Monwanou V.A. (2023): *Nonlinear dynamics of a nonlinear damping gyroscope and its passive control.*– J. Control. Sci. Engng., vol.2023, pp.1-17.

[6] Blekhman I.I. and Landa P.S. (2004): *Conjugate resonances and bifurcations in nonlinear systems under biharmonical excitation*.– Int. J. Non-linear Mech., vol.39, pp.421-426.

[7] Enjieu Kadji H.G. and Nana Nbendjo B.R. (2012): *Passive aerodynamics control of plasma instabilities*.– Commun. Nonlinear Sci. Numer. Simul., vol.17, pp.1779-1794.

[8] Siewe Siewe M., Moukam Kakmeni M.F. and Tchawoua C. (2004): *Resonant oscillation and homoclinic bifurcation in a Φ6-Van der Pol oscillator*.– Chaos Solit. Fract., vol.21, pp.841-853.

[9] Landa P.S. and McClintock P.V.E. (2000): *Vibrational resonance*.– J. Phys. A: Math. Gen., vol.l33, pp.433.

[10] Jeevarathinam C., Rajasekar S. and Sanjuan M.A.F. (2015): *Vibrational resonance in the Duffing oscillator with distributed time-delayed feedback.*– J. Appl. Nonlinear Dyn., vol.4, pp.1-15.

[11] Sarkar P. and Ray D.S. (2019)*: Vibrational anti-resonance in nonlinear coupled systems*.– Phs. Rev. E, vol. 99, pp.1-7.

[12] Roy-Layinde T.O., Laoye J.A., Popoola O.O. and Vincent U.E. (2016): *Analysis of vibrational resonance in bi-harmonically driven plasma*.– Chaos. vol.26, pp.1-9.

[13] Enjieu Kadji H.G., Nana Nbendjo B.R. Chabi Orou J.B. and Talla P.K. (2008): *Nonlinear dynamics of plasma oscillations modeled by an anharmonic oscillator.*– Phys. Plasmas., vol.15, pp.032308-1-032308-13.

[14] Ge Z. M. and Chen H.H. (1996): *Bifurcation and chaos in a rate gyro with harmonic excitation.*– J. Sound Vib., vol.194, pp.107-117.

[15] Miwadinou C.H., Monwanou V.A., Hinvi L.A., Tamba V.K., Koukpémèdji A.A. and Chabi Orou J.B. (2020): *Nonlinear oscillations of nonlinear damping gyros: resonances, hysteresis and multistability.*– Int. J. Bifur. Chaos, vol.30, pp.2050203-1-2050203-14.

[16] Leutcho G.D., Jafari S., Hamarash I.I., Kengne J., Tabekoueng Njitacke Z. and Hussain I. (2020): *A new megastable nonlinear oscillator with infinite attractors*.– Chaos Solitons and Fractals, vol.134, p.109703.

[17] Leutcho G.D., Khalaf A.J.M., Tabekoueng Njitacke Z., Fonzin Fozin T. Kengne J., Jafari S. and Hussain I. (2020): *A new oscillator with mega-stability and its Hamilton energy: infinite coexisting hidden and self-excited attractors*.– Chaos, vol.30, pp.033112-1.

[18] Tabekoueng Njitacke Z., Sami Doubla I., Tsafack N. and Kengne J. (2021): *Window of multistability and its control in a simple 3D Hopfield neural network: application to biomedical image encryption*.– Neural Comp. Appl., vol.33, pp.6733-6752.

[19] Leonov G.A. and Kuznetsov N.V. (2013): *Hidden attractors in dynamical systems. from hidden oscillations in Hilbert-Kolmogorov, Aizerman, and Kalman problems to hidden chaotic attractor in Chua circuits*.– Int. J. Bifur. Chaos, vol.23, pp.1330002-1330002-69.

[20] Rajagopal K., Takougang Kingni S., Kom G.H., Pham V.-T., Karthikeyan A. and Jafari S. (2020): *Self-excited and hidden attractors in a simple chaotic jerk system and in its time-delayed form: analysis, electronic implementation, and synchronization*.– J. Korean Phys. Soci., vol.77, pp.145-152.

[21] Chowdhury S.N., Ghosh D. (2020): *Hidden attractors: a new chaotic system without equilibria*.– European Phys. J. Special Topics, vol.229, p.6.

[22] Chowdhury S.N., Majhi S., Ghosh D., Prasad A. (2019): *Convergence of chaotic attractors due to interaction based on closeness*.– Physics Letters A, vol.383, p.125997.

[23] Chowdhury S.N., Kundu S., Perc M., Ghosh D. (2021): *Complex evolutionary dynamics due to punishment and free space in ecological multigames*.– Proceedings of the Royal Society A, vol.477, p.20210397.

[24] Chowdhury S.N., Banerjee J., Perc M. and Ghosh D. (2023): *Eco-evolutionary cyclic dominance among predators, prey, and parasites*.– Journal of Theoretical Biology, vol.564, p.111446.

[25] Aguessivognon J.M., Miwadinou C.H. and Monwanou A.V. (2023): *Effect of biharmonic excitation on complex dynamics of a two-degree-of-freedom heavy symmetric gyroscope*.– Phys. Scr., vol.98, p.095230.

[26] Chen H.K. (2002): *Chaos and chaos synchronization of a symmetric gyro with linear-plus-cubic damping*.– J. Sound Vib., vol.255, pp.719-740.

[27] Dooren R.V. (1996):*Comments on chaos and chaos synchronization of a symmetric gyros with linear – plus-cubic damping*.– J. Sound Vib., vol.268, pp.632-634.

[28] Xu Y., Lei W. and Zheng H. (2005): *Synchronization of two chaotic nonlinear gyros using active control*.– Phys. Let. A., vol.343, pp.153-158.

[29] Polo M.F.P. and Molina M.P. (2007): *A generalized mathematical model to analyze the nonlinear behavior of a controlled gyroscope in gimbals*.– Nonlinear Dyn., vol.48, pp.129-152.

[30] Asokanthan S.F. and Wang T. (2008): *Nonlinear instabilities in a vibratory gyroscope subjected to angular speed fluctuations*.– Nonlinear Dyn., vol.54, pp.69-78.

[31] Roopaei M., Zolghadri Jahromi M., John R. and Lin T.C. (2010): *Unknown nonlinear chaotic gyros synchronization using adaptive fuzzy sliding mode control with unknown dead-zone input*.– Commun. Nonlinear Sci. Numer. Simul., vol.15, pp.2536-2545.

[32] Aghababa M.P. and Aghababa H.P. (2013): *Chaos suppression of uncertain gyros in a given finite time*.– Chin. Phys. B., vol.21, p.110505.

[33] Loembe-Souamy R.M.D., Jiang G.P., Fan C.X. and Wang X.W. (2015): *Chaos synchronization of two chaotic nonlinear gyros using backstepping design*.– Math. Pro. Eng., vol.2015, p.850612.

[34] Kpomahou Y.J.F., Adomou A., Adéchinan J.A., Yamadjako A.E. and Madogni I.V. (2022): *Chaotic behaviors and coexisting attractors in a new nonlinear dissipative parametric chemical oscillator*.– Complexity, vol.2022, p.9350516.

[35] Kpomahou Y.J.F., Adomou A., Yamadjako A.E. and Djossou J. (2022): *Effect of amplitude-modulated force on horseshoe dynamics in Briggs-Rauscher chemical system modeled by a new parametric oscillator with asymmetric potential*.– European Phys. J. Plus., vol.137, p.679.

[36] Kpomahou Y.J.F., Adéchinan J.A., Ngounou A.M. and Yamadjako A.E. (2022): *Bursting, mixed-mode oscillations and homoclinic bifurcation in a parametrically and self-excited mixed Rayleigh-Liénard oscillator with asymmetric double well potential*.– Pramana, vol.96, p.176.

[37] Nourou Y., Miwadinou C.H., Agossou D.Y. and Monwanou A.V. (2024): *Effect of a parametric damping on nonlinear dynamics of a symmetric heavy gyroscope*.– Indian J. Phys., vol.98, pp.3623-3633, https://doi.org/10.1007/s12648-024-03095-6

Received: June 25, 2024
Revised: December 15, 2024